Supplementary Information

2′-Deoxyadenosine 5′-diphosphoribose is an endogenous TRPM2 superagonist

Ralf Fliegert[1], Andreas Bauche[1], Adriana-Michelle Wolf Pérez[1], Joanna M. Watt[2,3], Monika D. Rozewitz[1], Riekje Winzer[1], Mareike Janus[1], Feng Gu[1], Annette Rosche[1], Angelika Harneit[1], Marianne Flato[1], Christelle Moreau[2], Tanja Kirchberger[1], Valerie Wolters[1], Barry V.L. Potter[2,3,*], Andreas H. Guse[1,*]

*equal contribution

[1]The Calcium Signalling Group, Department of Biochemistry and Molecular Cell Biology, University Medical Centre Hamburg-Eppendorf, Martinistrasse 52, 20246 Hamburg, Germany

[2]Wolfson Laboratory of Medicinal Chemistry, Department of Pharmacy and Pharmacology, University of Bath, Bath, BA2 7AY, UK

[3]Medicinal Chemistry & Drug Discovery, Department of Pharmacology, University of Oxford, Mansfield Road, Oxford, OX1 3QT, UK

Supplementary Results

Supplementary Figure 1 – Adenine modified analogues

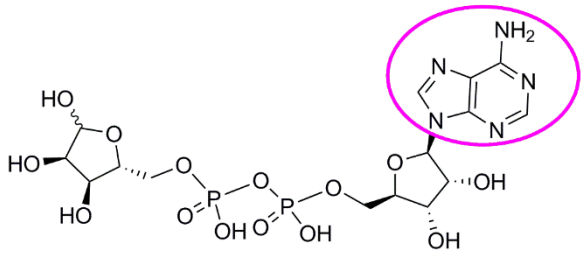

ADPR, **1**
adenosine 5'-diphosphoribose

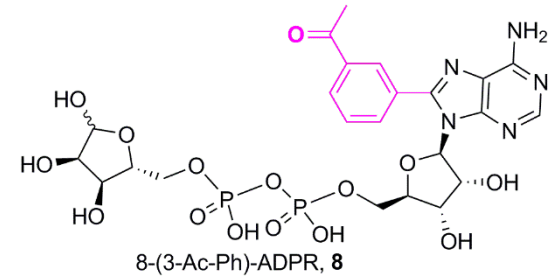

8-(3-Ac-Ph)-ADPR, **8**
8-(3-acetylphenyl)adenosine 5'-diphosphoribose

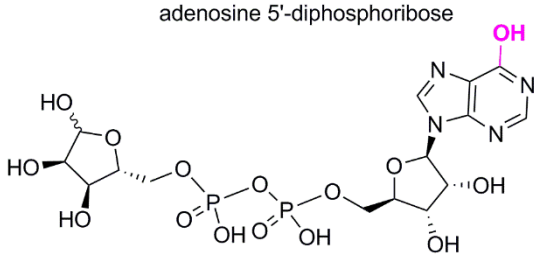

IDPR, **3**
inosine 5'-diphosphoribose

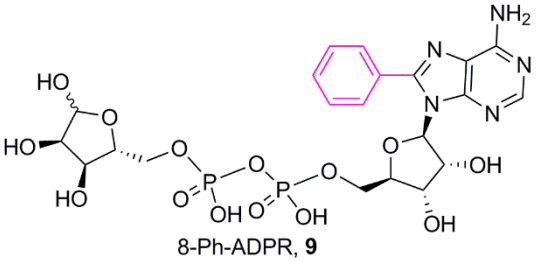

8-Ph-ADPR, **9**
8-phenyladenosine 5'-diphosphoribose

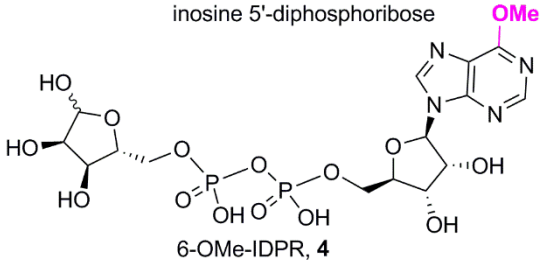

6-OMe-IDPR, **4**
6-*O*-methylinosine 5'-diphosphoribose

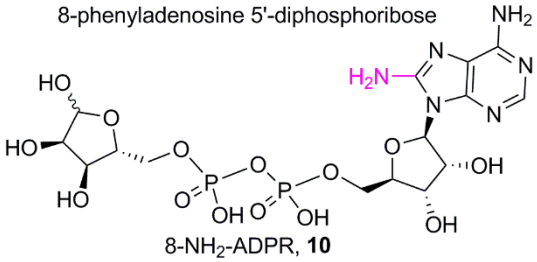

8-NH_2-ADPR, **10**
8-aminoadenosine 5'-diphosphoribose

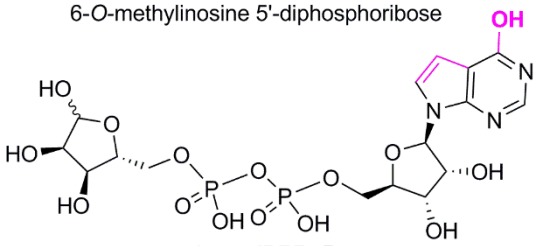

7-deaza-IDPR, **5**
7-deazainosine 5'-diphosphoribose

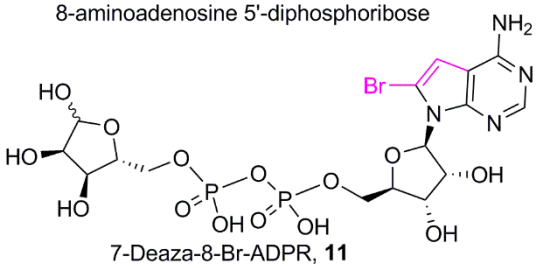

7-Deaza-8-Br-ADPR, **11**
7-deaza-8-bromoadenosine 5'-diphosphoribose

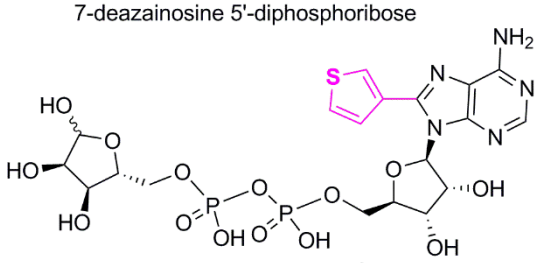

8-Thiophenyl-ADPR, **6**
8-(3-thiophenyl)adenosine 5'-diphosphoribose

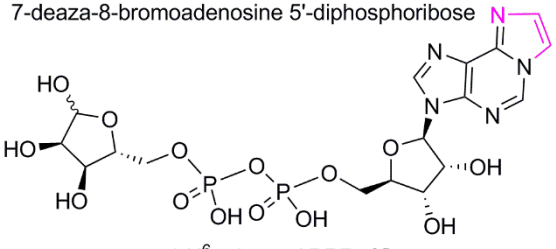

1,N^6-etheno-ADPR, **12**
1,N^6-ethenoadenosine 5'-*O*-diphosphoribose

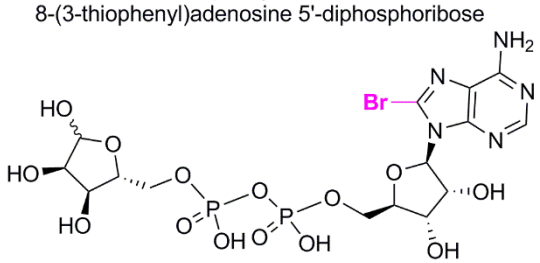

8-Br-ADPR, **7**
8-bromoadenosine 5'-diphosphoribose

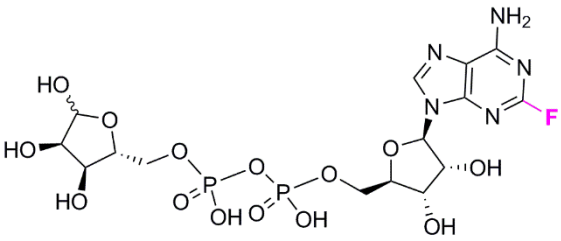

2-F-ADPR, **13**
2-fluoroadenosine 5'-diphosphoribose

Supplementary Figure 2 – Adenosine ribose modified analogues

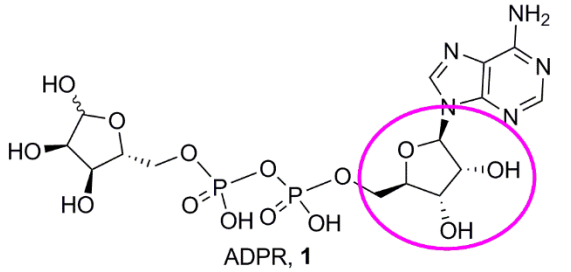

ADPR, **1**
adenosine 5'-diphosphoribose

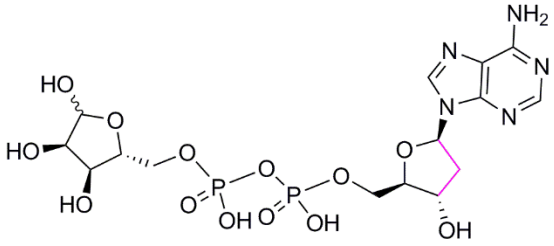

2'-deoxy-ADPR, **2**
2'-deoxyadenosine 5'-diphosphoribose

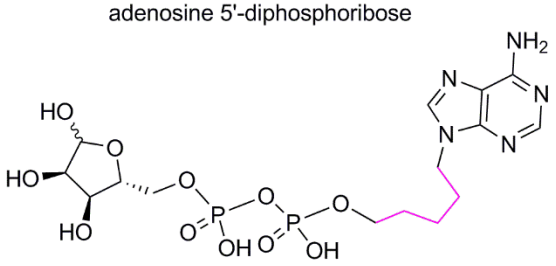

Acyclic-ADPR, **14**
acyclicadenosine 5'-diphosphoribose

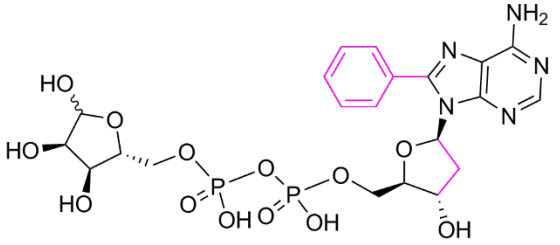

8-Ph-2'-deoxy-ADPR, **16**
8-phenyl-2'-deoxyadenosine 5'-diphosphoribose

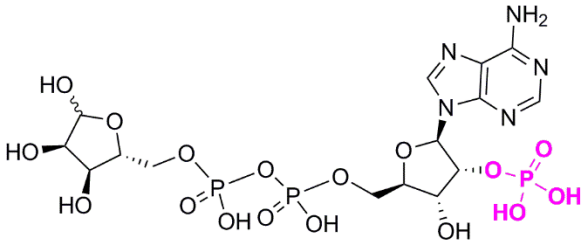

2'-Phospho-ADPR, **15**
2'-phosphoadenosine 5'-diphosphoribose

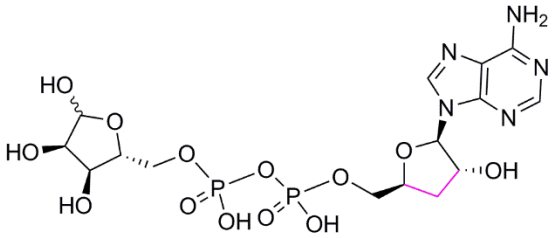

3'-deoxy-ADPR, **17**
3'-deoxyadenosine 5'-diphosphoribose

Supplementary Figure 3 – Pyrophosphate modified analogues

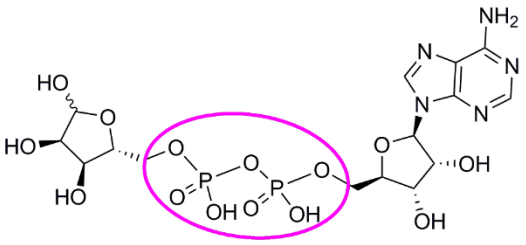

ADPR, adenosine 5'-diphosphoribose, **1**

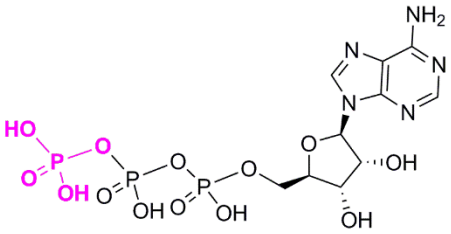

ATP, **18**
adenosine 5'-triphosphate

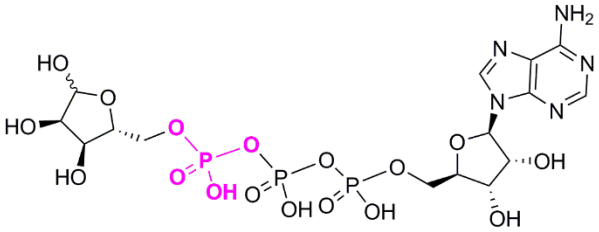

ATPR, **19**
adenosine 5'-triphosphate ribose

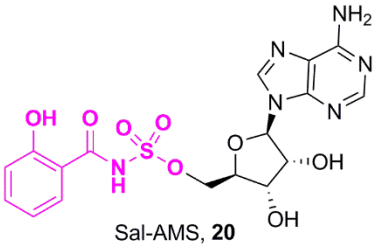

Sal-AMS, **20**
salicyclic adenosine monosulfamide

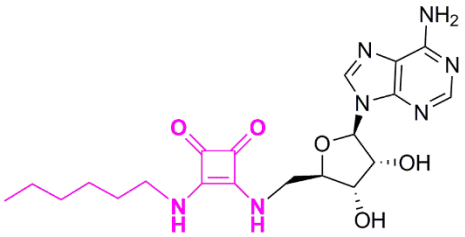

Hexyl-ASq, **21**
3-(5 -amino-5 -deoxyadenosine)-
4-(hexylamino)cyclobut-3-ene-1,2-dione

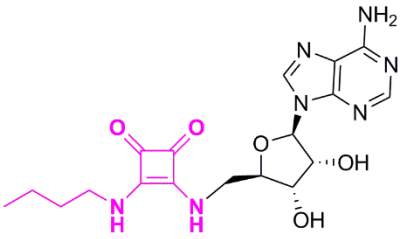

Butyl-ASq, **22**
3-(5 -amino-5 -deoxyadenosine)-
4-butylamino-cyclobut-3-ene-1,2-dione

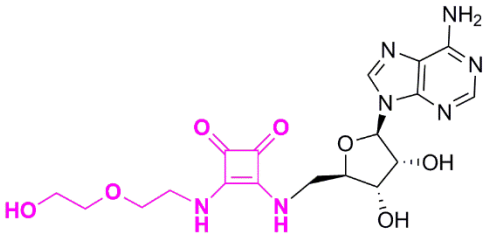

Hydroxy-ethoxy-ethyl-ASq, **23**
3-(5 -amino-5 -deoxyadenosine)-
4-(2-(2-hydroxyethoxy)ethylamino)cyclobut-3-ene-1,2-dione

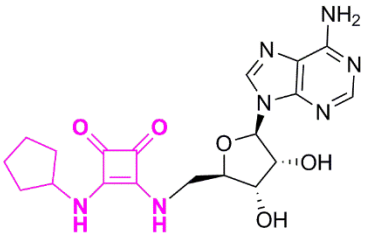

Cyclopentyl-ASq, **24**
3-(5-amino-5-deoxyadenosine)-
4-(cyclopentylamino)-cyclobut-3-ene-1,2-dione

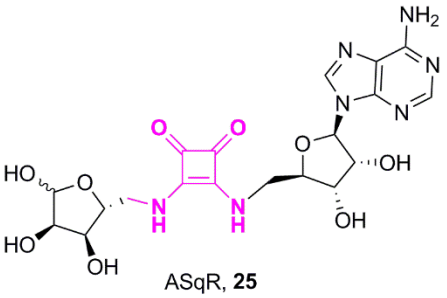

ASqR, **25**
3-(5 -amino-5 -deoxyadenosine)-4-(5-amino-5-deoxy-b-D-
ribofuranose)cyclobut-3-ene-1,2-dione

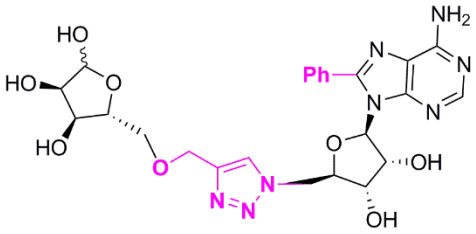

8-Ph-ATrR, **26**
8-phenyladenosine 1,4-triazole ribose,

Supplementary Figure 4 – Terminal ribose modified analogues

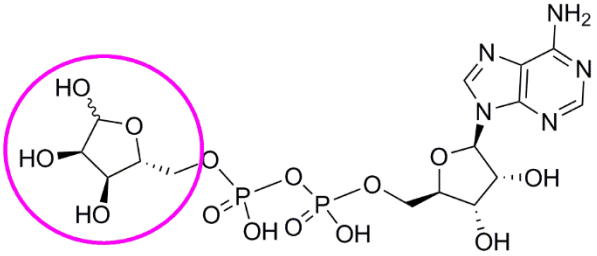

ADPR, **1**
adenosine 5'-diphosphoribose

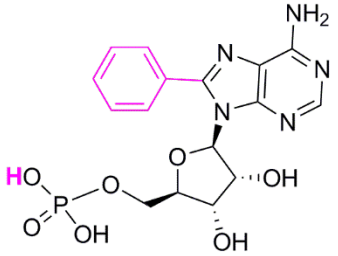

8-Ph-AMP, **31**
8-phenyladenosine 5'-monophosphate

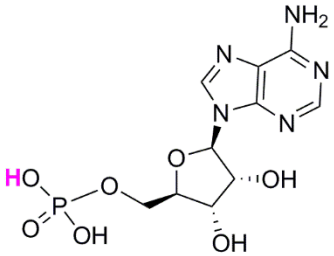

AMP, **27**
adenosine 5'-monophosphate

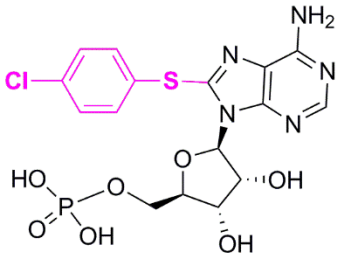

8-pCPT-AMP, **32**
8-(4-chlorophenylthio)adenosine
5'-monophosphate

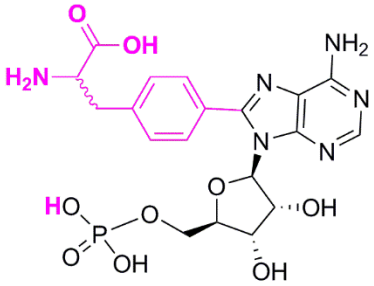

8-(4-Ph-ala)-AMP, **28**
8-(4-(2-aminopropanoic acid)phenyl)adenosine
5'-monophosphate

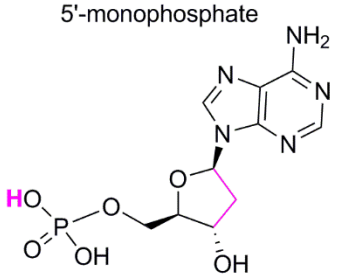

2'-deoxy-AMP, **33**
2'-deoxyadenosine 5'-monophosphate

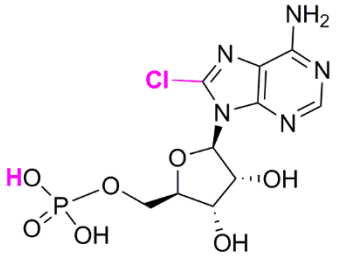

8-Cl-AMP, **29**
8-chloroadenosine 5'-monophosphate

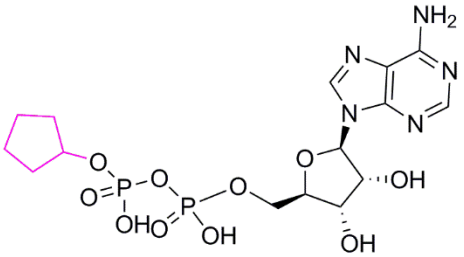

Cyclopentyl-ADP, **34**
β-cyclopentyladenosine 5'-diphosphate

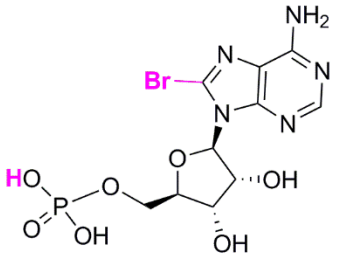

8-Br-AMP, **30**
8-bromoadenosine 5'-monophosphate

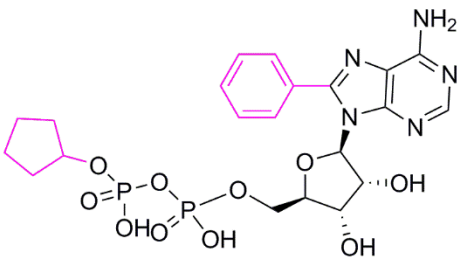

Cyclopentyl-8-Ph-ADP, **35**
β-cyclopentyl-8-phenyladenosine 5'-diphosphate

Supplementary Figure 5

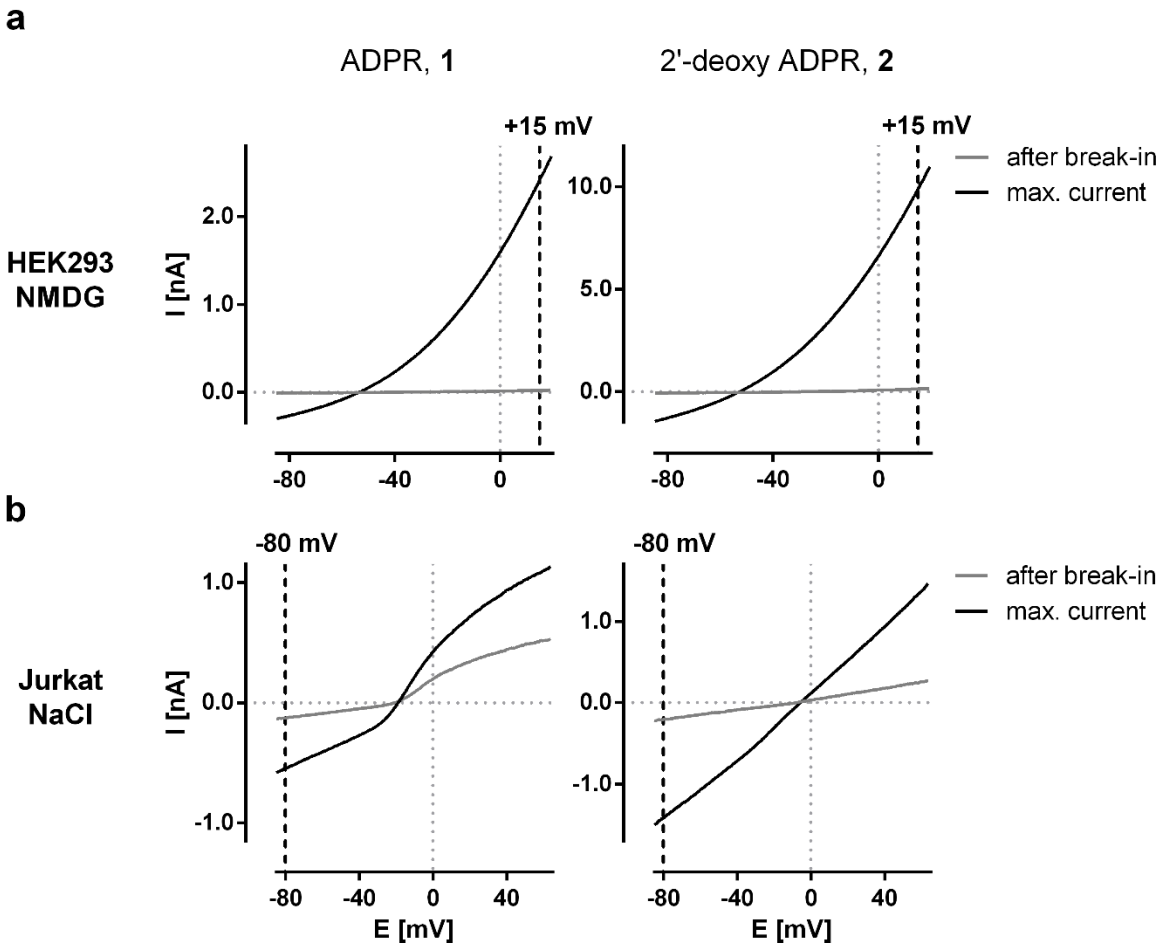

I-V curves for human TRPM2 activated by either ADPR or 2′-deoxy-ADPR derived from voltage ramps. a I-V curves from whole cell patch clamp experiments with HEK293 cells expressing hTRPM2 in NMDG-based bath solution. Shown are average I-V curves from single voltage ramps of individual cells (ADPR: 14 cells, 2′-deoxy-ADPR: 8 cells) directly after break-in to whole-cell configuration (gray line) or at maximum amplitude (black line). Since TRPM2 is impermeable to NMDG the I-V relationship is distinctly non-linear with the outward current more pronounced than the inward current. The quantification of currents (Fig. 2a+c) has therefore been determined at +15 mV (dashed line). The panels for ADPR and 2′-deoxy-ADPR were scaled to show the similarity in the shape of the curve, note the difference in the max. current. **b** Whole cell patch clamp experiments with wild type Jurkat cells in physiological ionic conditions (NaCl/KCl). Shown are average I-V curves directly after break-in to whole-cell configuration (gray line) or at maximum current over the period from 300s (black line, ADPR: 8 cells, 2′-deoxy-ADPR: 4 cells). For Jurkat cells there is a current component from voltage-gated potassium channels already visible directly after break-in. The difference between the maximum current ramp and the ramp

directly after break-in has the expected linear I-V relationship for a non-selective cation channel like TRPM2. The quantification of currents (Fig 2b) has been determined at –80 mV (indicated by dashed line).

Supplementary Figure 6

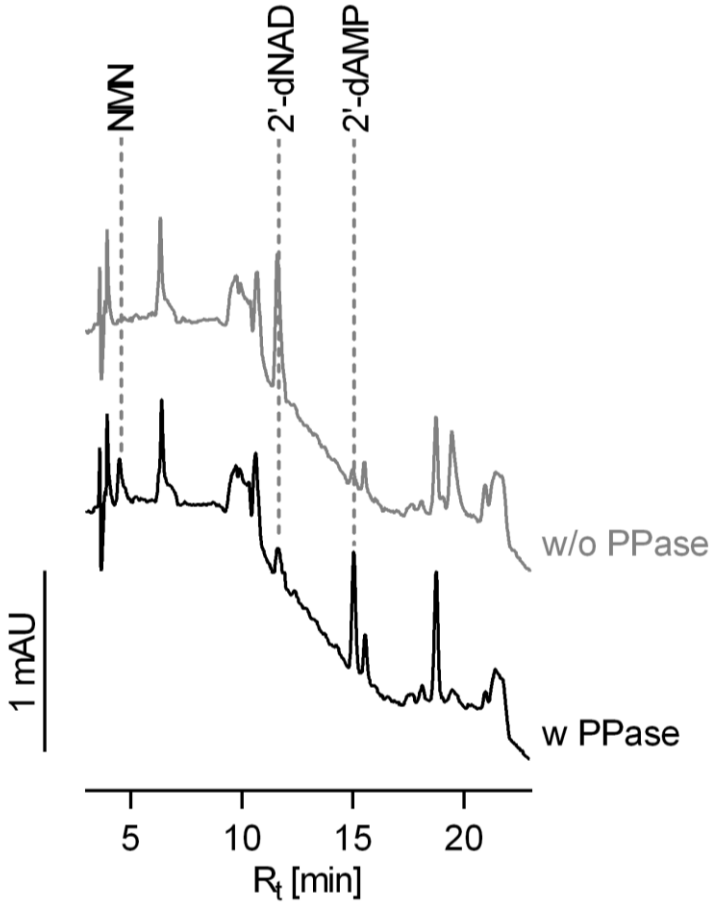

Nucleotide pyrophosphatase cleaves the reaction product of NMNAT-2 into 2'-deoxy-AMP and NMN. NMNAT-2 was incubated with β-nicotinamide 5′-mononucleotide (NMN, 290 µmol/L) and 2'-deoxy-ATP (2.5 mmol/L) for 15 min at 37°C. During analysis of the reaction products by HPLC (Fig. 4a), the peak co-eluting with authentic 2'-deoxy-NAD was collected and subjected to hydrolysis by nucleotide pyrophosphatase from *Crotalus adamanteus* to yield the expected product 2'-deoxy-AMP.

Supplementary Figure 7

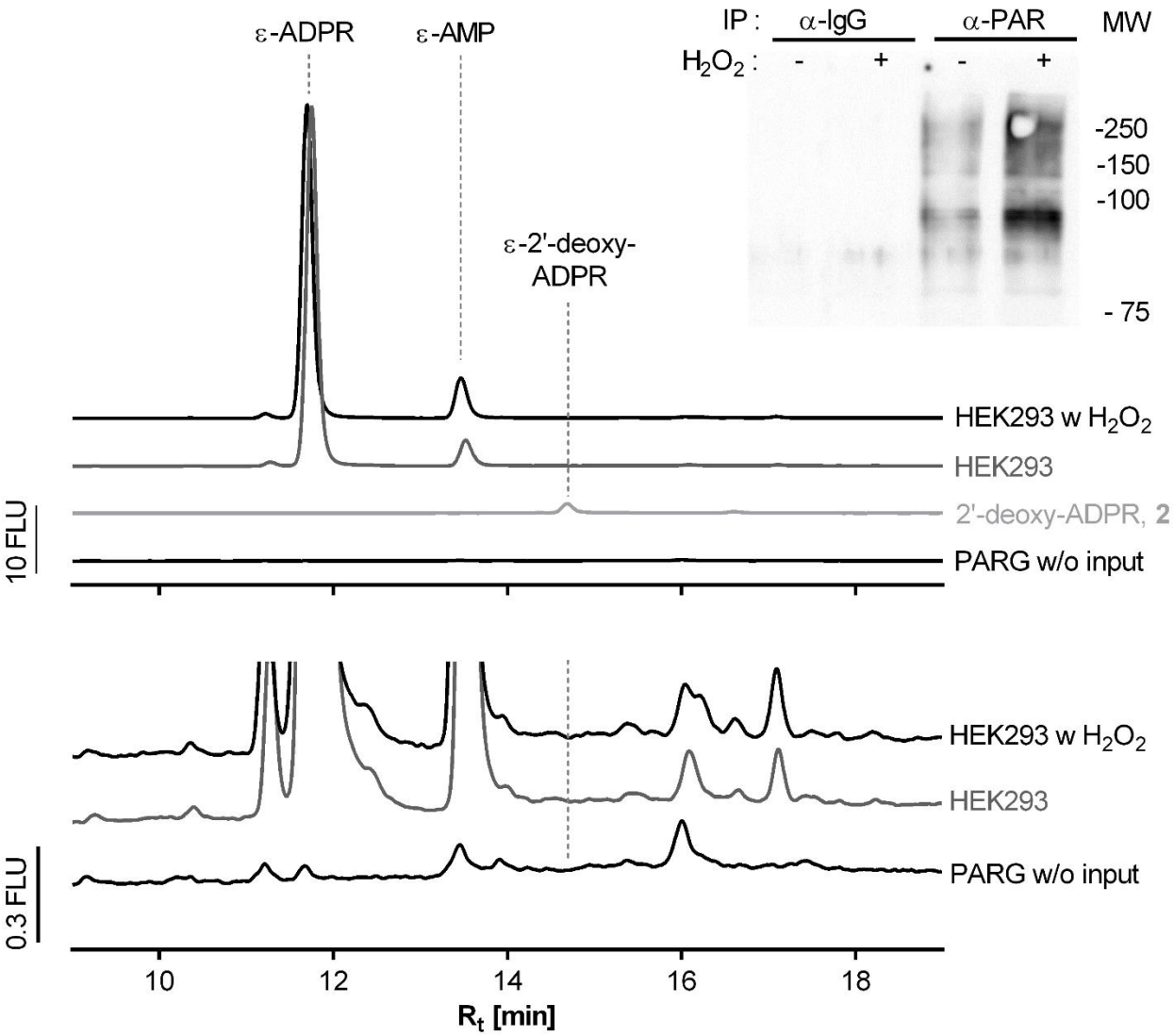

Hydrolysis of poly-ADP ribose chains of poly ADP ribosylated proteins by recombinant Poly (ADP-ribose) glycohydrolase (PARG) does not produce detectable amounts of 2′-deoxy-ADPR. Poly ADP ribosylated proteins from HEK293 cells (unstimulated or exposed to 1 mM H_2O_2 for 5 min were isolated by immunoprecipitation using an anti poly-ADPR antibody (10H). As control normal mouse IgG was used instead of the anti-PAR antibody. The upper inset shows the result of Western Blot analysis using another primary antibody against poly-ADPR (anti-PAR from rabbit) and a HRP-conjugated goat anti-rabbit secondary antibody confirming precipitation of ADP-ribosylated proteins (Supplementary Fig. 14). The amount of poly-ADP ribosylated proteins increased after exposure to hydrogen peroxide (representative for 3 independent experiments). Poly-ADP ribosylated proteins from immunoprecipitation were incubated with 100

ng recombinant PARG enzyme (2.5 h at 37°C). After passing them through 10kDa cutoff centrifugal filters, samples were incubated for 40 min at 80°C with chloroacetaldehyde to turn adenine compounds to the respective 1, N^6-etheno derivatives. The products were analyzed by reverse phase HPLC on a BDS Multohyp C18 column. Fluorescence allowed for specific detection of 1, N^6-etheno derivatives of adenine nucleotides (excitation 230 nm, emission 410 nm). Despite the high sensitivity (40 fmol with S/N ratio $\geq$ 3) 1, N^6-etheno-2′-deoxy-ADPR could not be detected.

Supplementary Figure 8

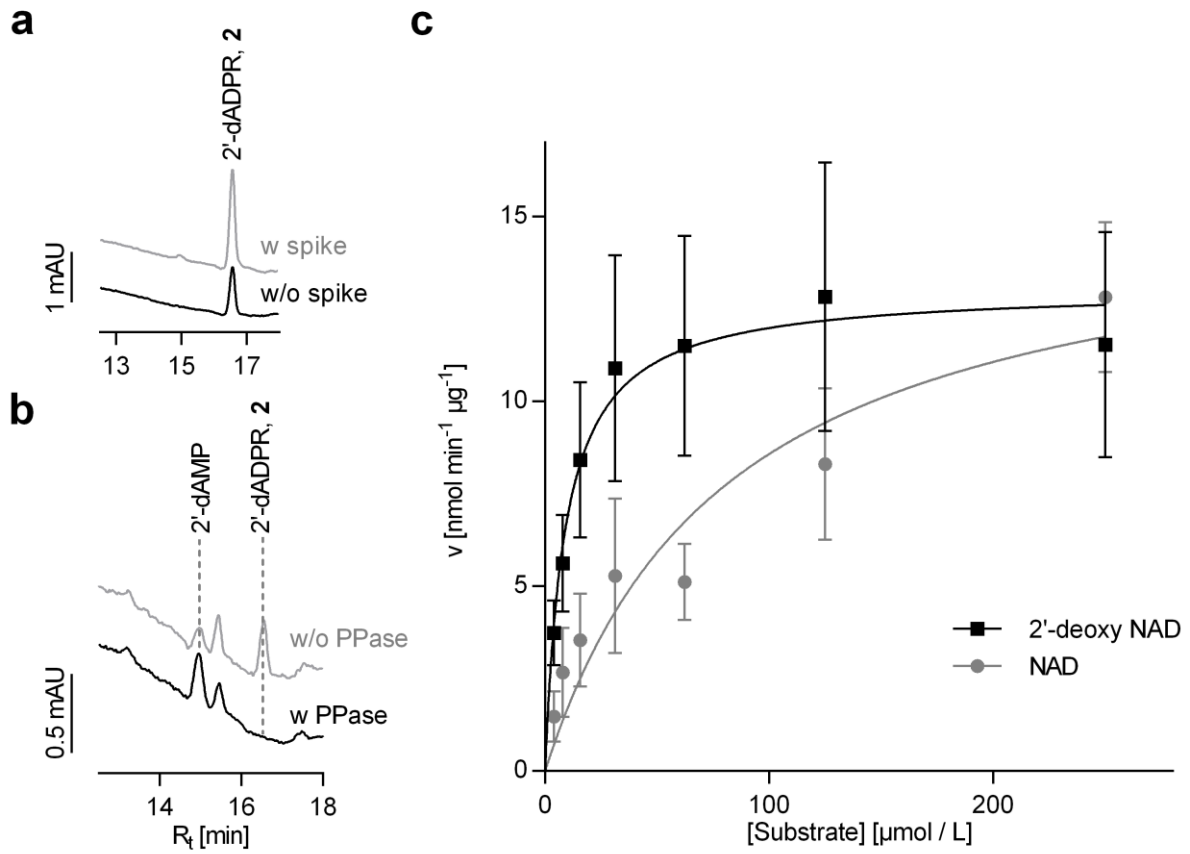

CD38 hydrolyzes 2'-deoxy-NAD to yield 2'-deoxy-ADPR *in vitro*. During analysis of the reaction products of CD38 by HPLC (Fig. 4c), the peak co-eluting with authentic 2'-deoxy-ADPR was collected. **a,** To confirm identity of this product, samples were spiked with authentic 2'-deoxy-ADPR, or, **b,** were hydrolyzed by nucleotide pyrophosphatase from *Crotalus adamanteus* (60 min at 37°C*)* to yield 2'-deoxy-AMP. Reaction products were analyzed by ion-pair RP-HPLC. Chromatograms in panels a + b are representative of 3 independent experiments **c,** Saturation plot for NAD and 2'-deoxy-NAD as substrates of soluble recombinant hCD38. hCD38 (0.5 – 1.0 ng) was incubated with increasing concentrations of either NAD or 2'-deoxy-NAD at 37°C. Initial reaction rates were calculated from the amount of product formed, as determined by HPLC. Data were fitted to Michaelis-Menten models (data are shown as mean±SEM from three experiments for NAD (n=3 for each data point) and four experiments for 2'-deoxy-NAD (n=4 for each data point).

Supplementary Figure 9

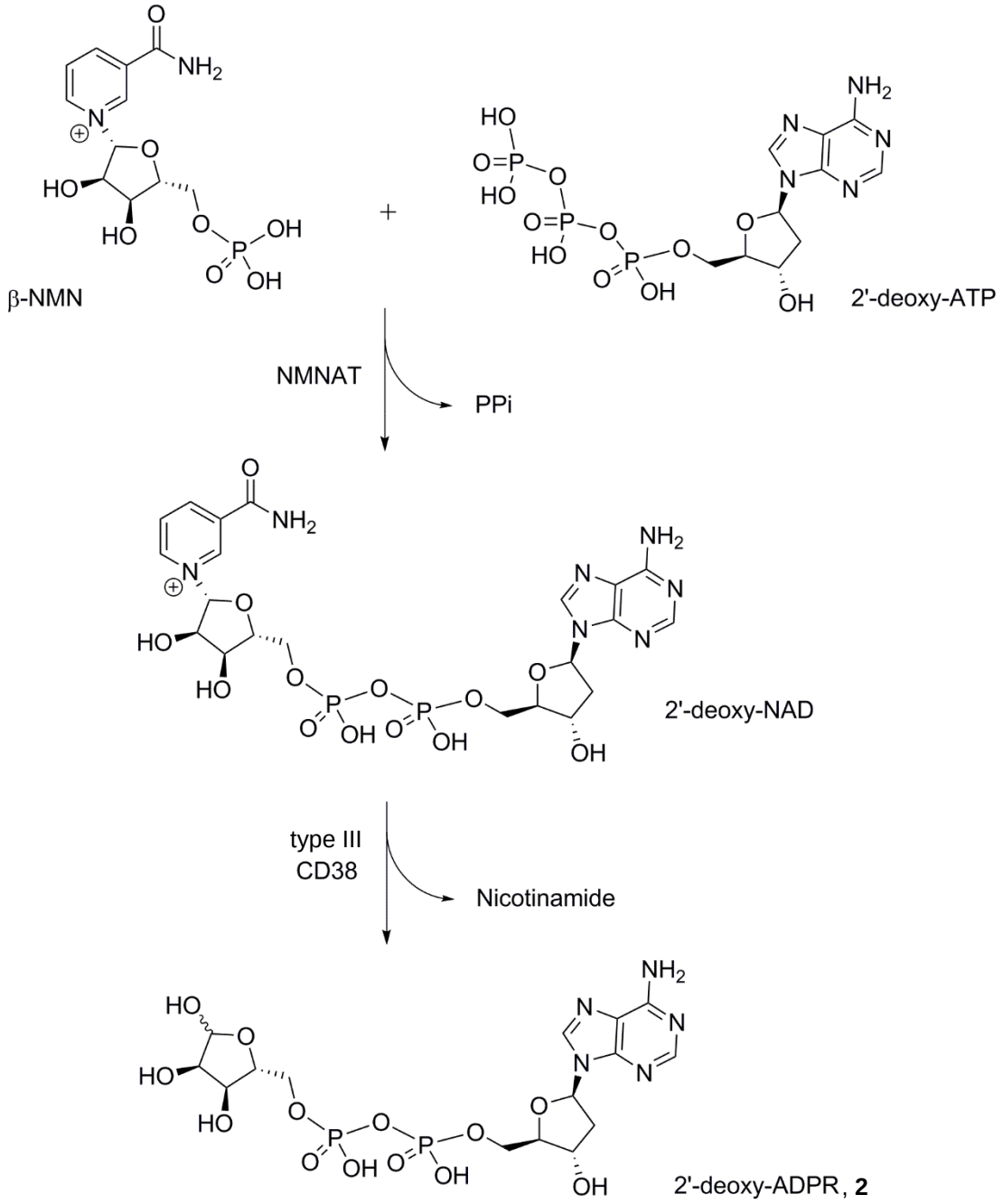

Proposed pathway for biosynthesis of 2′-deoxy-ADPR by NMNAT-2 and CD38.

Supplementary Figure 10

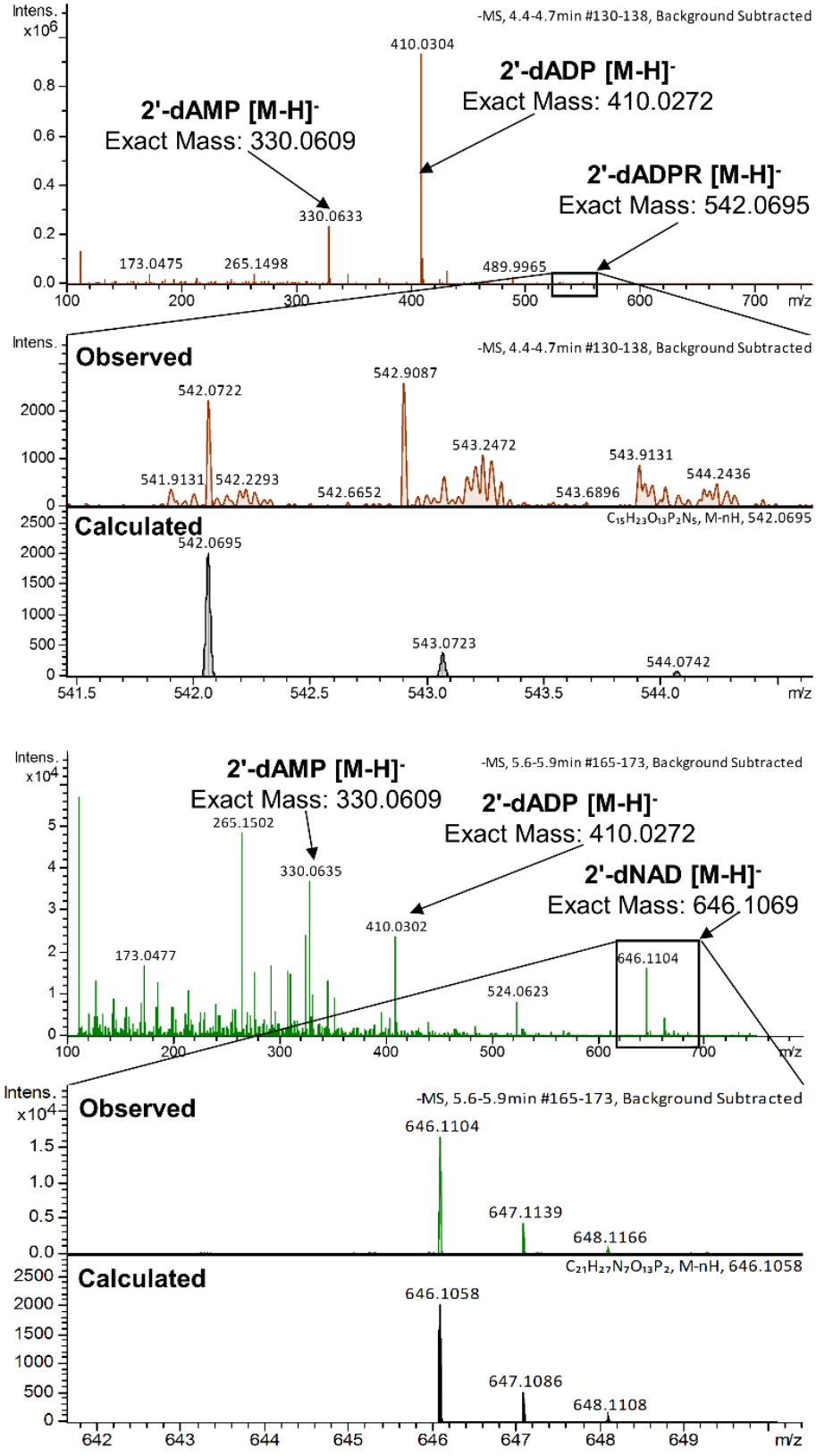

2′-deoxy-ADPR and 2′-deoxy-NAD detected in samples from Jurkat cells by mass spectrometry a + b Peaks of 2′-deoxy-ADPR and 2′-deoxy-NAD collected after two-step-HPLC

were freeze dried to remove volatile buffer components and submitted to ultrahigh resolution ESI-QTOF mass spectrometry in negative mode. The molecular ion and expected ^{13}C isotopic pattern was observed (lower panel), as well as the fragmentation products 2′-deoxy-ADP and 2′-deoxy-AMP.

Supplementary Figure 11

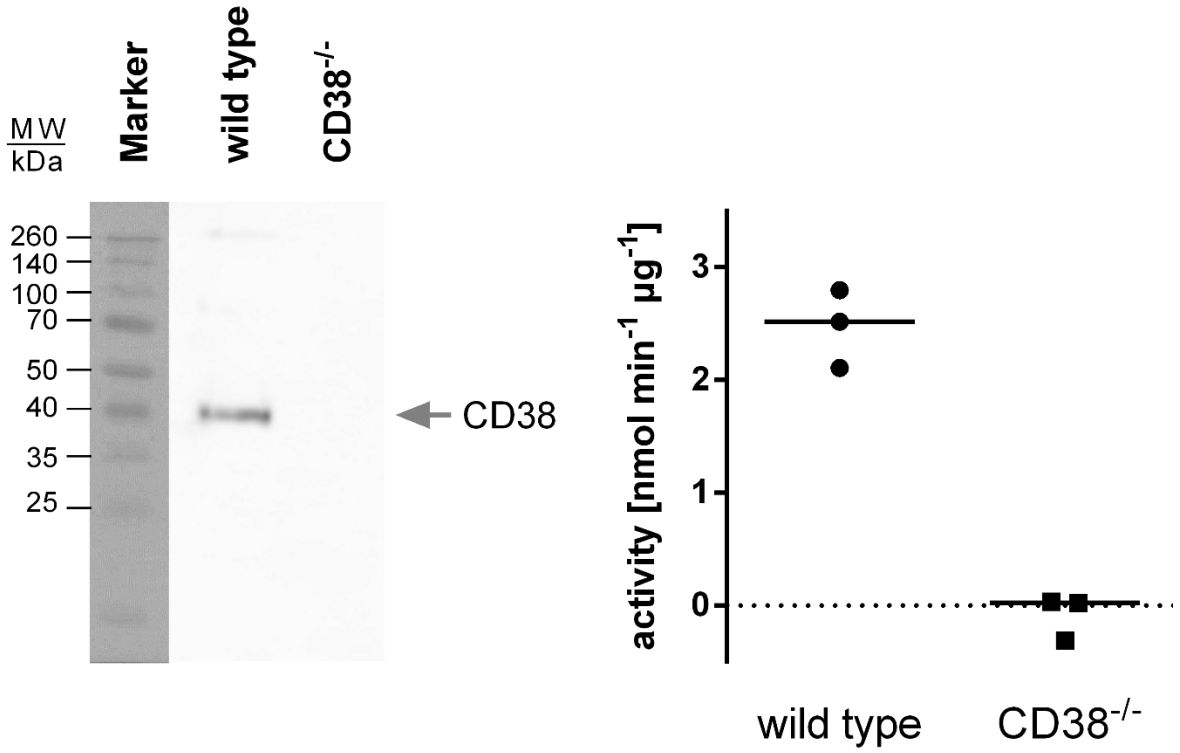

CD38 protein expression and NAD glycohydrolase activity was not detectable after knock-out of CD38 in Jurkat cells. To confirm knock-out of CD38 by CRISPR/Cas9 technology, P10 membranes were prepared from the generated Jurkat cell line as detailed in the methods section. **a** CD38 protein expression was analyzed by western blot using the anti-CD38 antibody AT-1 (Supplementary Fig. 15). Whereas CD38 was clearly detectable as a single band at 40 kDa in the wild type cells, no such band was visible in the knock-out cells (representative for three independent membrane preparations and blots). **b** NAD glycohydrolase activity was determined using 1,N^6-etheno-NAD as substrate as detailed in the Methods section. Data from three independent membrane preparations are shown with the horizontal line indicating the median. Whereas the median activity in wild type cells was 2.5 nmol min^{-1} μg^{-1} (median, IQR: 2.1 – 2.8 nmol min^{-1} μg^{-1}), there was no detectable enzyme activity in $CD38^{-/-}$ cells.

Supplementary Figure 12

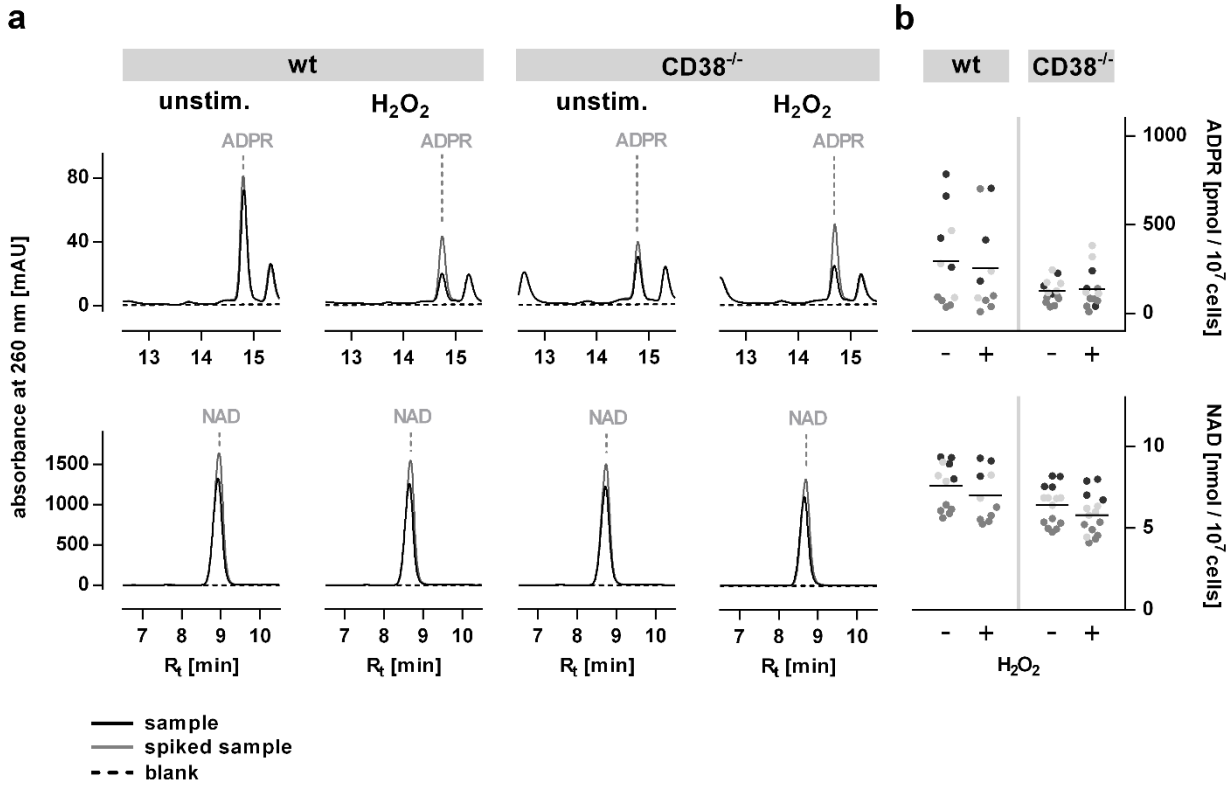

Endogenous ADPR and NAD are not significantly affected by knock-out of CD38 in Jurkat cells. Jurkat cells and cells of a Jurkat cell line with CRISPR/Cas9-mediated knock-out of CD38 were either exposed to 100 µmol/L H_2O_2 for 5 min or left unstimulated. Deproteinized extracts from these cells were separated by RP-HPLC on C 8 column and fractions co-eluting with ADPR or β-NAD were collected. These fractions were separated in a second dimension of RP-HPLC on C18 column. To correctly assign peaks even in the presence of small shifts in retention time, each sample was split and one half was spiked with the respective standard nucleotide (light gray lines). **a** Representative chromatograms for each condition from a single experiment are shown. **b**, Quantitative analysis of the impact of H_2O_2 on intracellular ADPR and β-NAD. Independent experiments were initiated on 3 separate days over the course of one month, with each experiment consisting of multiple parallel cell preparations. 2–6 data points were obtained per experimental day. Results from single experiments are indicated as filled circles (horizontal lines indicate the

mean) with the same shade of gray signifying individual experiments from a single day. Data are normally distributed in each group (D'Agostino-Pearson Omnibus Normality Test, α=0.05). Analysis by one-way ANOVA followed by multiple comparison using Sidak's correction for multiple testing did not reveal significant differences for ADPR (adj. p-values = 0.62 and 0.78 for simulated vs unstimulated and 0.11 / 0.12 for wildtype vs $CD38^{-/-}$) or β-NAD (adj. p-values = 0.98 / 0.99 for stimulated vs unstimulated and 0.11 / 0.44 for wildtype vs $CD38^{-/-}$).

Supplementary Figure 13

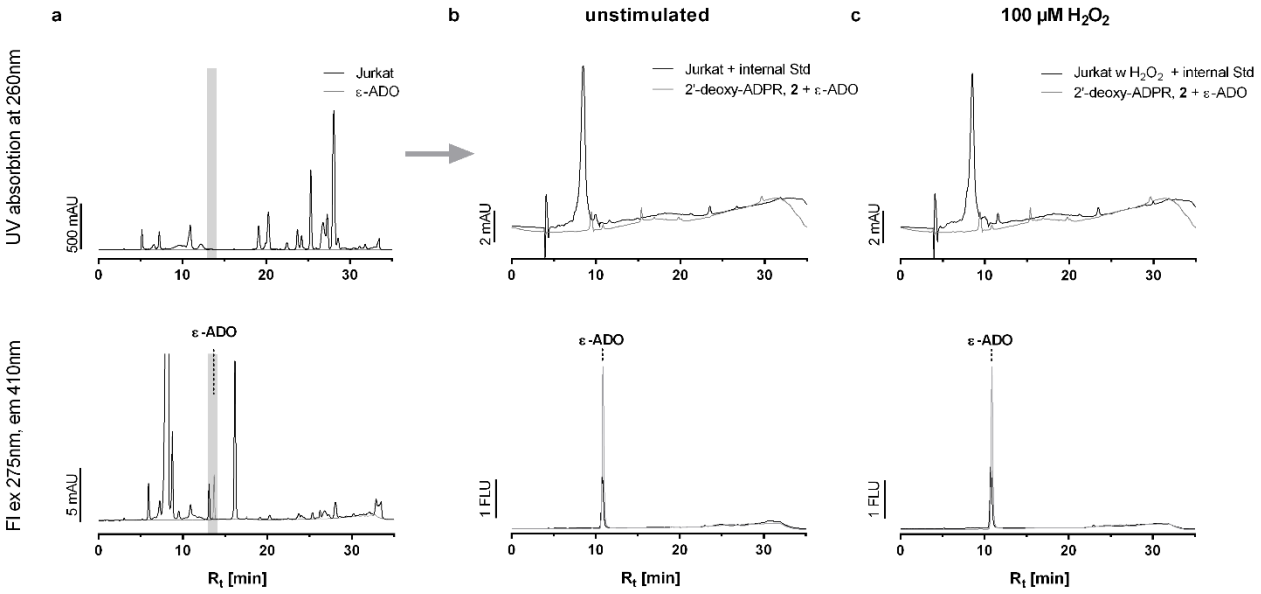

1, N^6-ethenoadenosine was used as internal standard for the determination of recovery during two-step HPLC analysis of endogenous 2′-deoxy-ADPR in Jurkat cells a, Fluorescent 1, N^6-ethenoadenosine was added to deproteinized cell extracts from either unstimulated Jurkat cells or Jurkat cells exposed to 100 µM H_2O_2, before they were applied to a Phenomenex Luna C8 5 µ column. Fractions co-eluting with 1, N^6-ethenoadenosine (R_t between 13 and 14 min, indicated as shaded area) and with chemically synthesized 2′-deoxy-ADPR (R_t between 24 and 25 min, s. shaded area in Fig. 4a) were collected separately. The particular example shown here is from the same experiment as in Fig. 4. For the detection of adenine nucleotides light absorption at 260 nm (top chromatograms) was recorded using a DAD (diode array detector, Agilent Technologies). for 1,N^6-Ethenoadenosine was detected using an FAD (fluorescence detector, Agilent Technologies) with excitation at 275 nm and emission at 410 nm (bottom chromatograms) **b + c,** The fractions co-eluting with 1,N^6-ethenoadenosine were re-chromatographed on a Multohyp BDS-C18 5 µ column. 1,N^6-Ethenoadenosine was quantified using a three point calibration curve. The calculated recovery for 1,N^6-ethenoadenosine was used to correct quantification of 2′-deoxy ADPR.

Supplementary Figure 14

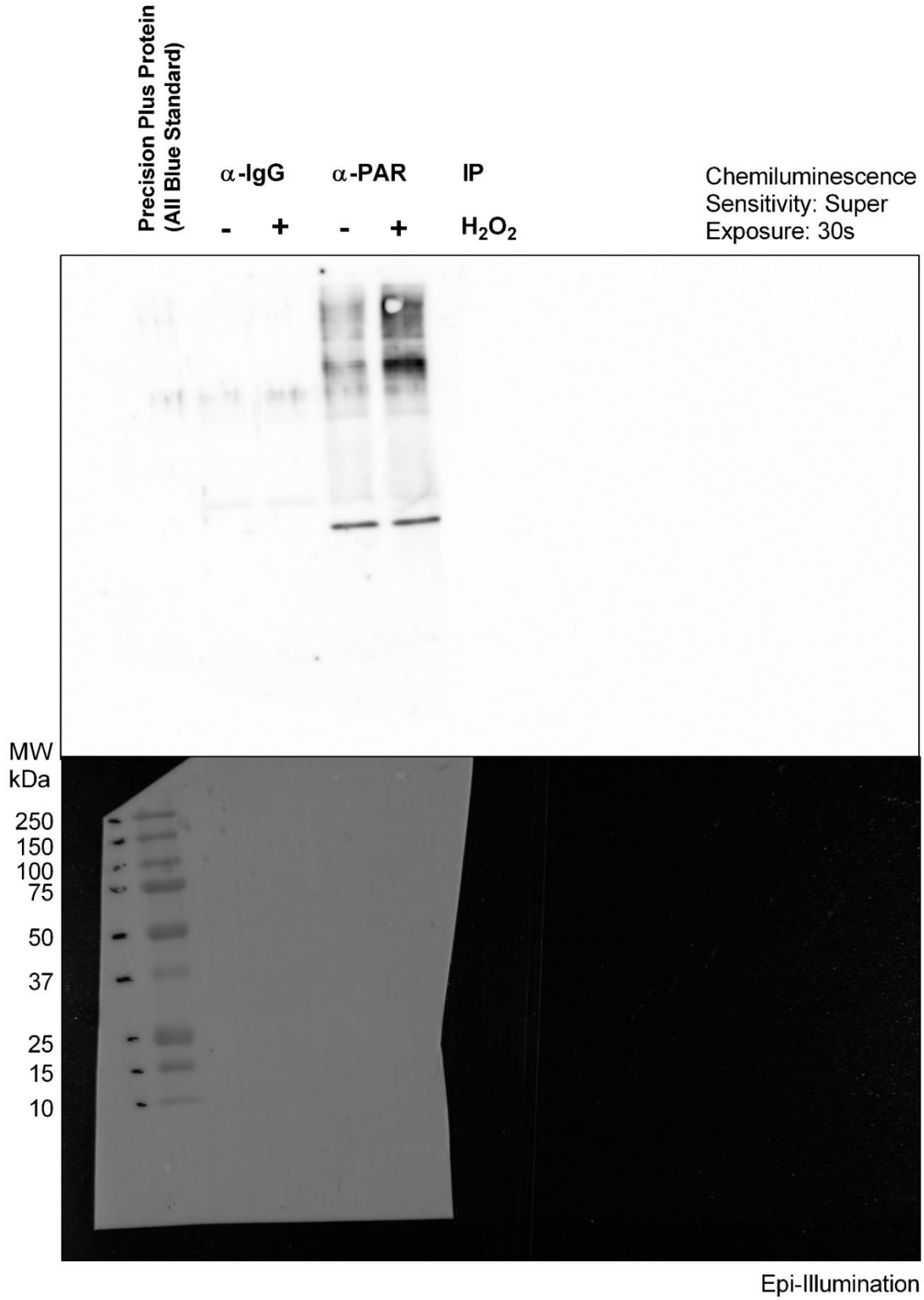

Full chemiluminescence and epi-illumination images of the WesternBlot shown in Supplementary Figure 7

Supplementary Figure 15

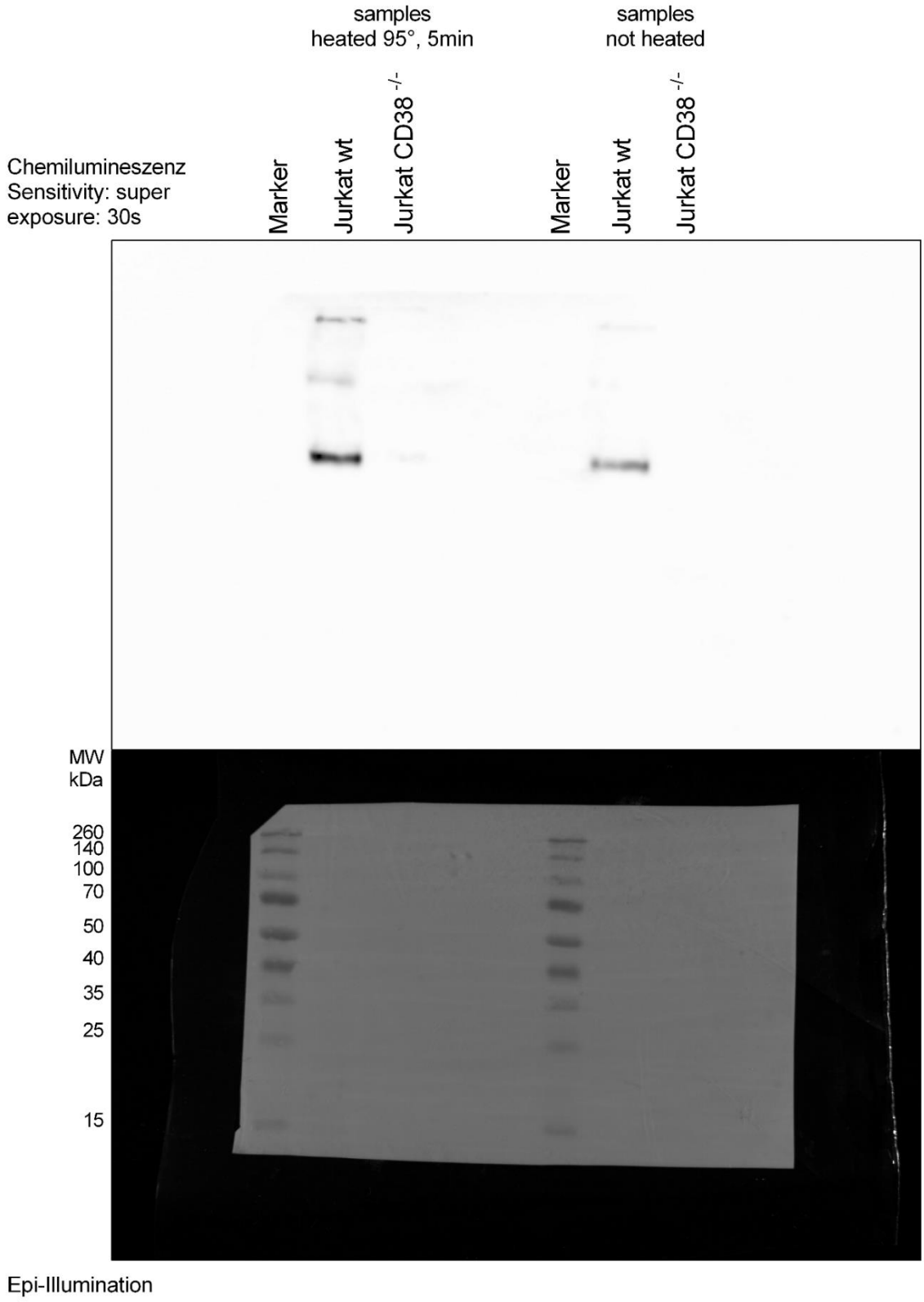

Full chemiluminescence and epi-illumination images of the WesternBlot shown in Supplementary Figure 11